Chemical Engineering and Processing 74 (2013) 115–123

Contents lists available at ScienceDirect

Chemical Engineering and Processing: Process Intensification

journal homepage: www.elsevier.com/locate/cep

Ultrasound assisted synthesis of polythiophene/SnO_2 hybrid nanolatex particles for LPG sensing

S.S. Barkade[a], D.V. Pinjari[b], U.T. Nakate[c], A.K. Singh[c,1], P.R. Gogate[b], J.B. Naik[a], S.H. Sonawane[d,*], A.B. Pandit[b]

[a] University Department of Chemical Technology, North Maharashtra University, Jalgaon 425001, India
[b] Chemical Engineering Department, Institute of Chemical Technology, Mumbai 400 019, India
[c] Nanomaterials and Sensors Lab., Defence Institute of Advanced Technology (DU), Girinagar, Pune 411025, India
[d] Department of Chemical Engineering, National Institute of Technology, Warangal 506004, India

ARTICLE INFO

Article history:
Received 14 August 2012
Received in revised form 15 August 2013
Accepted 15 September 2013
Available online 20 September 2013

Keywords:
Ultrasound
Hybrid latex oxidative polymerization
Polythiophene/SnO_2 hybrid nanocomposite
LPG sensor
p–n Heterojunction

ABSTRACT

Polythiophene (PTP) coated SnO_2 nano-hybrid particles have been synthesized using an ultrasound assisted in situ oxidative polymerization of thiophene monomers. Reference experiments have also been performed in the absence of ultrasound to clearly illustrate the effect of ultrasonic irradiations. FTIR results show broadening and shifting of peaks toward lower wave numbers, suggesting better conjugation and chemical interactions between PTP and SnO_2 particles. Due to strong synergetic interaction between the SnO_2 nanoparticles and polythiophene, this hybrid nanocomposite has the potential application as chemical sensors. It has been observed that PTP/SnO_2 hybrid sensors could detect liquefied petroleum gas (LPG) with high sensitivity at room temperature. PTP/SnO_2 hybrid composite containing 20 wt% SnO_2 showed the maximum sensitivity at room temperature. The sensing mechanism of PTP/SnO_2 hybrid nanocomposites to LPG was mainly attributed to the effects of p–n heterojunction between PTP and SnO_2.

1. Introduction

Organic–inorganic hybrid core–shell nanoparticles are being used in number of engineering applications due to versatile functional properties of the organic and inorganic constituents. These core–shell particles often exhibit significant improvement in magnetic, optical and electrical properties, which make them attractive for both scientific and technological applications in the different areas such as catalysis, coatings, drug delivery, optics, electronics, biology etc. [1–3]. Encapsulation of the inorganic materials by the various polymer matrices, or the immobilization of the inorganic phase on the surface of the polymer particles can be used to prepare core–shell morphology of the nanocontainers. Immobilization can be physical or chemical in nature leading to varying extents of bonding strength between the two different phases. To achieve the compatibility of phases, inorganic particles are pre-dispersed in the continuous phase. The ultrasound assisted miniemulsion chemical oxidative polymerization in the presence of inorganic particles leads to the formation of hybrid particles if the interaction between the two phases is controlled. The conditions of ultrasound assisted polymerization process can be optimized for achieving a nanoscale dispersion containing inorganic particles and these hybrid functional nanomaterials could be utilized for specific applications [4].

Ultrasonically induced cavitation can generate local temperatures as high as 5000 K and local pressures as high as 1000 atm, with local heating and cooling rates greater than 10^9 K/s [5]. In this environment, water molecule dissociates into primary hydrogen radicals ($H^{\bullet}$) and hydroxyl radicals ($OH^{\bullet}$) in a collapsing cavitation bubble. Subsequently, these active species take part in driving the polymerization reactions. Also, ultrasonic irradiations help in creating the hybrid nanoparticles with their synergetic or complementary behaviors that are not observed in their single counterparts. The benefits of the ultrasound include narrow size distribution, high purity, unique reaction effects, higher yields, and the ability to form nanoparticles with uniform shapes [6–8]. Because of its ability to produce the hybrids with significantly beneficial properties, the use of ultrasound has shown a rapid growth in material science. These novel surface properties of the hybrid can play a crucial role in gas sensing applications and hence the present work has concentrated on synthesis of a hybrid material with possible potential for gas sensing application.

There have been some earlier studies reporting the use of hybrid materials for gas sensor applications. The

* Corresponding author. Tel.: +91 870 2462626.
E-mail addresses: shirishsonawane09@gmail.com, shirishsonawane@rediffmail.com (S.H. Sonawane).
[1] Center for Piezoceramics and Devices, ARDE, Defence Research and Development Organisation (DRDO), Pune.

0255-2701/$ – see front matter © 2013 Elsevier B.V. All rights reserved.
http://dx.doi.org/10.1016/j.cep.2013.09.005

drawbacks of conventional synthesis methods like higher reaction temperature, lower kinetic reaction rates, higher amount of initiator, low yields and selectivity can be overcome by the use of ultrasound due to the enhanced physical and chemical effects of acoustic cavitation in the heterogeneous systems [9–14]. Ram et al. [15] prepared polyhexythiophene/SnO_2 and poly(ethylenedioxythiophene)/SnO_2 composite thin films, which showed an excellent sensitivity to NO_2 at concentration of ppb levels. It was reported that the hybrid materials exhibit much higher sensitivity and better selectivity as compared to the pure inorganic and organic materials. Dhawale et al. [16] found that the polyaniline/TiO_2 sensor presented maximum response of 63% upon exposure to 0.1 vol% liquefied petroleum gas (LPG) in air at room temperature. Nicho et al. [17] developed a polyaniline composite sensor useful for detection of low concentrations of NH_3 gas. Hosono et al. [18] prepared intercalated polyaniline/MoO_3 hybrids, which showed good sensing characteristics for the VOCs. Many authors have investigated gas sensing properties of conducting polymer-SnO_2 hybrid composites for different gases like acetone, ethanol, methanol, NH_3, NO_x and hydrogen sulfide. However, there is not a single report about application of thiophene-SnO_2 hybrid composite for LPG sensing at room temperature. LPG is highly flammable and even at low level concentration (ppm), it becomes a serious threat to human lives. Due to this and significant usage in cooking/automobile application, it is imperative that fast and selective detection of LPG is necessary to avoid any leakage of gas, which can help in preventing the occurrence of accidental explosions.

In the present work, core shell hybrid materials have been prepared with SnO_2 nanoparticles as the core and polythiophene (PTP) as the shell using an ultrasound assisted in situ chemical oxidative polymerization. The cavitating conditions like local intense micromixing, high temperature/pressure pulse can be very helpful in getting the desired properties for the synthesized nanoparticles [19–25]. Initially SnO_2 nanoparticles have been synthesized in the presence of ultrasonic irradiations and later these have been used for preparation of hybrid material again in the presence of ultrasound. XRD and FTIR analysis have been performed to demonstrate possible synergetic interaction between PTP and SnO_2 nanoparticles. Gas sensing properties of the synthesized hybrid material to LPG have been systematically studied. The possible sensing mechanism of PTP/SnO_2 hybrid has also been discussed.

2. Materials and methods

2.1. Materials

Tin tetrachloride ($SnCl_4{\cdot}5H_2O$) and urea ($(NH_2)_2CO$) of analytical grade and reagent grade ferric chloride were procured from Central Drug House, India. Thiophene was procured from Merck whereas chloroform ($CHCl_3$) and methanol (CH_3OH) were obtained from Sigma Aldrich. All the chemicals were used as received from the supplier.

2.2. Synthesis of SnO_2 nanoparticles in the presence of ultrasound

In the preparation of SnO_2 nanoparticles, 0.1 M aqueous solution of tin tetrachloride and urea has been utilized as starting materials. Synthesis was carried out by mixing tin tetrachloride and urea solutions in a ratio of 1:2 using ultrasonic horn with an operating frequency of 22 kHz and rated output power of 750 W. The mixture was irradiated for 1 h on 5 s pulse mode (5 s on and 5 s off mode). The standard depth of immersion of the horn in the solution was 1 cm and it was located at the center of the glass reactor to achieve the maximum cavitation [26]. The system was operated with 50% amplitude, giving theoretical energy dissipation rate as 375 W (0.50 × 750 = 375 W). The calorimetric efficiency of the ultrasonic horn, as measured in the current work, was about 12.8% giving actual energy dissipation in the liquid as 38.4 W. The white precipitate was separated by centrifugation at 6000 rpm for 30 min. Further, the final product was washed with distilled water several times and dried in an oven at 90 °C. The obtained SnO_2 nanoparticles were ground using mortar and pestle and finally calcined at 600 °C for 2 h.

2.3. Synthesis of SnO_2 encapsulated polythiophene hybrid via ultrasound assisted in situ chemical oxidative polymerization

The PTP/SnO_2 hybrids were prepared via ultrasound assisted in situ chemical oxidative polymerization using anhydrous $FeCl_3$ as the oxidant in batch mode (Fig. 1). The experimental setup consists of a reactor which is mainly a jacketed glass vessel of 400 mL volume capacity equipped with a 13 mm stainless steel probe connected to an ultrasonic generator.

In a typical synthesis, 0.052 g of SnO_2 was uniformly dispersed in 100 mL of chloroform in the reactor equipped with ultrasonic horn [27,28]. The irradiation time was 20 min in order to keep them in dispersed form in the solution. Then, 1 mL of thiophene monomer was added drop wise in the reactor and the mixture was sonicated for 20 min to achieve adsorption of the thiophene monomers on the surface of SnO_2. Further, oxidant $FeCl_3$ solution with a mole ratio of $FeCl_3$/Thiophene (2:1) was added, followed by sonication for 40 min. Reaction mixture was heated after addition of $FeCl_3$, and the temperature was maintained at 40 °C (±1 °C) throughout the duration of the experiment. The complete reaction was carried over a period of 60 min in the presence of ultrasonic irradiation to ensure complete encapsulation of the SnO_2 in the polymer latex. The color of the mixture changes from gray to black. The product was filtered and washed with methanol several times. During washing, the color of the product changed from black to red [29]. The final product was dried at 60 °C under vacuum for 12 h. By the same method, a series of PTP/SnO_2 hybrids varying in loading of SnO_2 were prepared and designated as PTP/(5%)SnO_2, PTP/(10%)SnO_2, PTP/(15%)SnO_2 and PTP/(20%)SnO_2. Also pure PTP was synthesized in the absence of SnO_2 by a similar procedure. Synthesis of hybrid PTP/SnO_2 nanocomposite with different loading of SnO_2 was also prepared via the conventional approach (in the absence of ultrasound) of chemical oxidative polymerization with an objective of establishing the role of ultrasound.

2.4. Characterization

X ray diffraction (XRD) pattern of pure SnO_2 and PTP/SnO_2 was recorded using powder X-ray diffractometer (XRD, Philips Xipert Pro PW-3040). The size and morphology of the nanoparticles of SnO_2 embedded into the polythiophene matrix was determined using a transmission electron microscope (TEM, JEOL JSM2000-EX II). An infrared (IR) spectrum of samples was also obtained using a SHIMADZU 8400S FTIR spectrometer in KBr medium at room temperature in the region of 4000–500 cm^{-1}. Particle size distribution analysis of SnO_2 encapsulated polythiophene was carried out by Photon Correlation Spectroscopy (PCS, 3000 HAS, analyzer Malvern). The weight loss of pure SnO_2 and hybrid nanocomposite was determined in the range of 30 to 600 °C using thermogravimetric analysis (PerkinElmer TGA system, USA), at a heating rate of 10 °C/min.

2.5. Gas sensor fabrication using PTP/SnO_2 hybrid

The PTP/SnO_2 hybrid was pressed into pellet form of diameter ~1.4 cm, thickness ~0.1 cm and the electrical contact leads were fixed at a distance of 1 cm with the help of silver paste on the

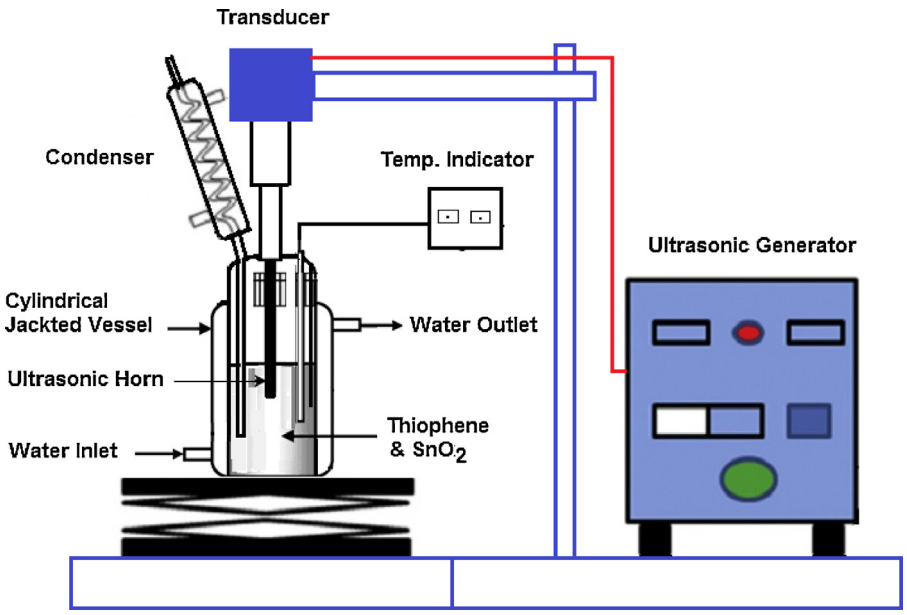

Fig. 1. Experimental setup for synthesizing polythiophene coated SnO_2 nano hybrid via ultrasound assisted chemical oxidative polymerisation.

surface of the pellet to form sensing element. LPG sensing experiments were carried out in a static gas chamber under ambient conditions. The sensing element was kept on a glass base which holds the sensing element tightly. The sensing measurements were performed by exposing the sensor (as pellets) to LPG in a closed glass dome (25 L) using a two probe method. The known volume of the LPG was introduced into the gas chamber filled with air and it was maintained at atmospheric pressure. Gas sensing setup comprises a temperature controller, K type thermocouple, an electrically heated plate, gas chamber and volume measurement unit [30]. The performance of the sensing element is presented in terms of the gas response (S), which is defined by the relation:

$$S = \frac{(R_g - R_a)}{R_a} \times 100$$

where R_a and R_g are values of the sensor resistance in air and in the presence of LPG, respectively.

3. Results and discussion

3.1. Mechanism of formation of PTP/SnO_2 hybrid using ultrasound assisted in situ chemical oxidative polymerization

PTP coated SnO_2 nanoparticles were successfully synthesized using ultrasound assisted in situ polymerization of thiophene monomers in chloroform using anhydrous $FeCl_3$ (oxidant and dopant) [31,32,24]. The process of formation of hybrid material is illustrated in Fig. 2. Initially, the reaction media containing SnO_2 nanoparticles, chloroform and thiophene is sonicated in order to adsorb thiophene monomer molecules on the surface of SnO_2 nano particles. After introducing anhydrous $FeCl_3$ into the reactor in the presence of ultrasound, polymerization of thiophene is initiated. In the initiation stage, radicals are generated through deprotonation of cation which is formed by the complexation between the thiophene sulfur, $FeCl_3$ and water molecules due to the cavitational effects generated by acoustic cavitation [33]. These free radicals enter the thiophene monomer droplets resulting into polymerization process. The radicals also accelerate the rate of thiophene polymerization and conversion. Due to ultrasound cavitation fast dissociation of the oxidant molecule takes places. Uniform size monomer droplets are formed due to violent shearing action produced by acoustic cavitation. The physical effects of intense turbulence and liquid circulation currents due to cavitation results into a rapid dispersion of nano-sized SnO_2 into the monomer droplets [6].

During polymerization, SnO_2 nano particles are surrounded by oxidized polythiophene [34]. The polythiophene shell becomes thin due to the extraction of the iron chloride. During this process, the color changes from gray (oxidized state) to red (reduced state). Complete removal of gray color was achieved by the filtration of product and washing with methanol several times. During washing, the color of the product changed from black to red.

3.2. FTIR analysis of SnO_2 and PTP/SnO_2 hybrid nanocomposites

Fig. 3 shows the FTIR spectra of SnO_2 nanoparticles, pure PTP and PTP/SnO_2 hybrid material. For pure PTP, there are various weak peaks in the range of 2800–3100 and 1690 cm^{-1}, which can be attributed to the C–H stretching vibrations and C=C characteristic peak, respectively. In the finger print region of PTP, the IR absorption peak at 787 cm^{-1} was recognized due to the C–H out of plane stretching vibration of the 2,5-substituted thiophene ring, which confirmed the polymerization of thiophene monomer. The absorption peak at 698 cm^{-1} is assigned to the C–S bending mode, which indicates the presence of thiophene monomer [35,36]. The infrared spectra of PTP/SnO_2 hybrid show almost identical wave numbers and positions in the range of 500–4000 cm^{-1} compared to that of the pure PTP, but in Fig. 3(b), the peak intensity reduced and a new peak appeared at around 700 cm^{-1} demonstrating the presence of SnO_2 [37]. It is clear that, as compared to the peak at 685 cm^{-1} reported in Fig. 3(a) of SnO_2, the peak of the hybrid is shifted to higher wavenumber (700 cm^{-1}). It clearly indicates that strong synergic interaction exists between SnO_2 and sulfur atom of the thiophene linkage [38,39]. The broadening and changes in peak positions suggest that a strong chemical interaction between PTP and SnO_2 is responsible to change the polymer conformation. It is expected that the presence of ultrasound may play a vital role in better dispersion of nano SnO_2 particles into polythiophene, creating a strong adhesion [40–42].

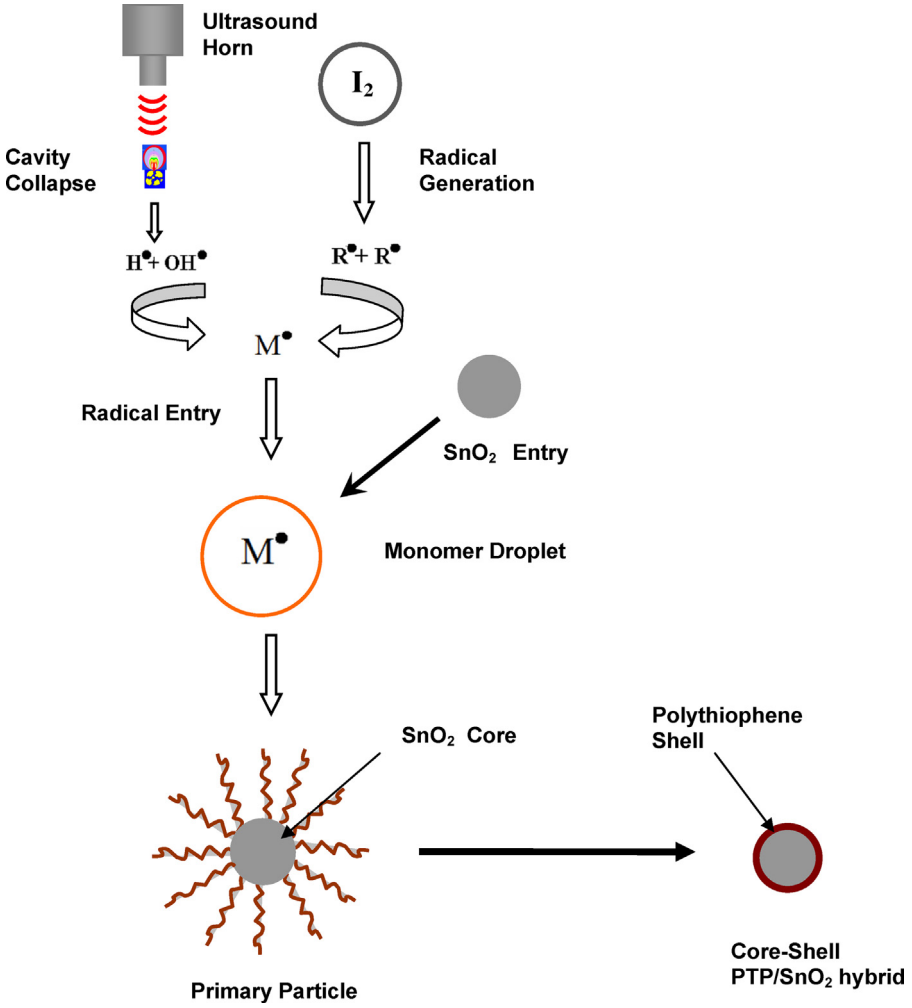

Fig. 2. Schematic illustration of the formation of polythiophene coated SnO_2 nano hybrid via ultrasound assisted chemical oxidative polymerisation.

3.3. *X-ray diffraction analysis and TEM analysis of SnO_2 and PTP/SnO_2 hybrids*

Fig. 4 shows the XRD patterns of the SnO_2, pure PTP and PTP/(10%) SnO_2 hybrid materials. All the peaks appeared in SnO_2 XRD diffractogram match well with the standard SnO_2 tetragonal rutile structure (JCPDS:41-1445). For PTP, the XRD pattern showed a broad, amorphous diffraction peak at approximately $2\theta = 20^\circ$–24° as depicted in Fig. 4(a). It indicates the existence of polythiophene, which is in accordance with the previous report [43]. The peak centered around 22.8°, corresponds to the intermolecular π–π stacking for the pure thiophene [44]. For PTP/(10%) SnO_2 hybrids, all the major peaks existing in the pure SnO_2 were also observed, but the peaks were weaker than those of the SnO_2, which may have resulted from the possible interaction between PTP and SnO_2 [45]. After addition of SnO_2 in the nanocomposite, the XRD peak gets shifted from 24° to 30°. It is attributed to induced strain in the polymer nanocomposite due to incorporation of SnO_2 in polythiophene by ultrasound assisted in situ chemical oxidative polymerization method.

The morphology of the SnO_2 and PTP/SnO_2 hybrid prepared by ultrasound assisted chemical oxidative polymerization is reported in Fig. 5(a) and (b) respectively. The diameter of the SnO_2 nanoparticles is about 15–20 nm. The TEM image of the PTP/SnO_2 hybrid shows that all SnO_2 nanoparticles are encapsulated by PTP, and no uncovered SnO_2 nanoparticles are observed. The SnO_2 nanoparticles are dispersed uniformly in PTP, which can potentially be attributed to the ultrasonic irradiation used during polymerization, which may break the aggregation of SnO_2 nanoparticles. The problem of effective dispersion of SnO_2 nanoparticles into the polythiophene arising from their very high surface energy is expected

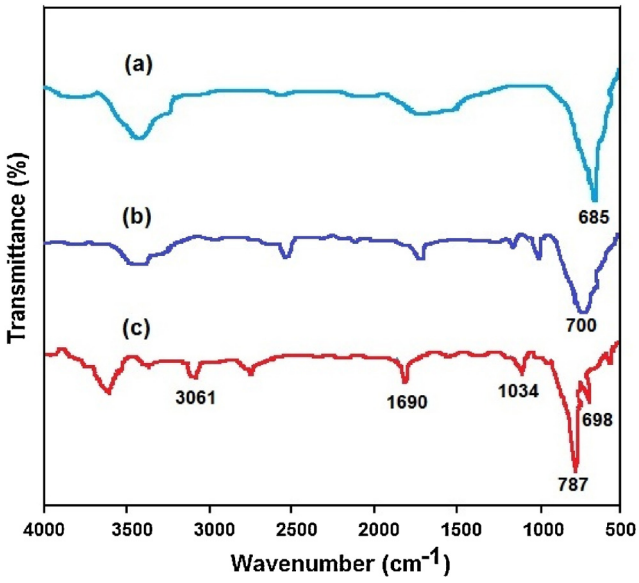

Fig. 3. FTIR spectra of nano size (a) SnO_2, (b) PTP/SnO_2 hybrid and (c) pure PTP.

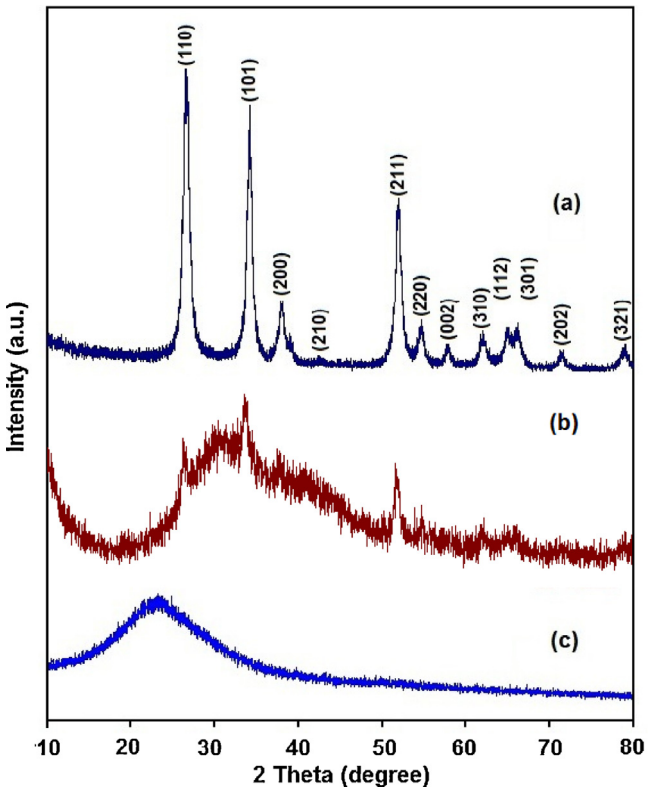

Fig. 4. X-ray diffraction of nano size (a) SnO_2, (b) PTP/SnO_2 hybrid and (c) pure PTP.

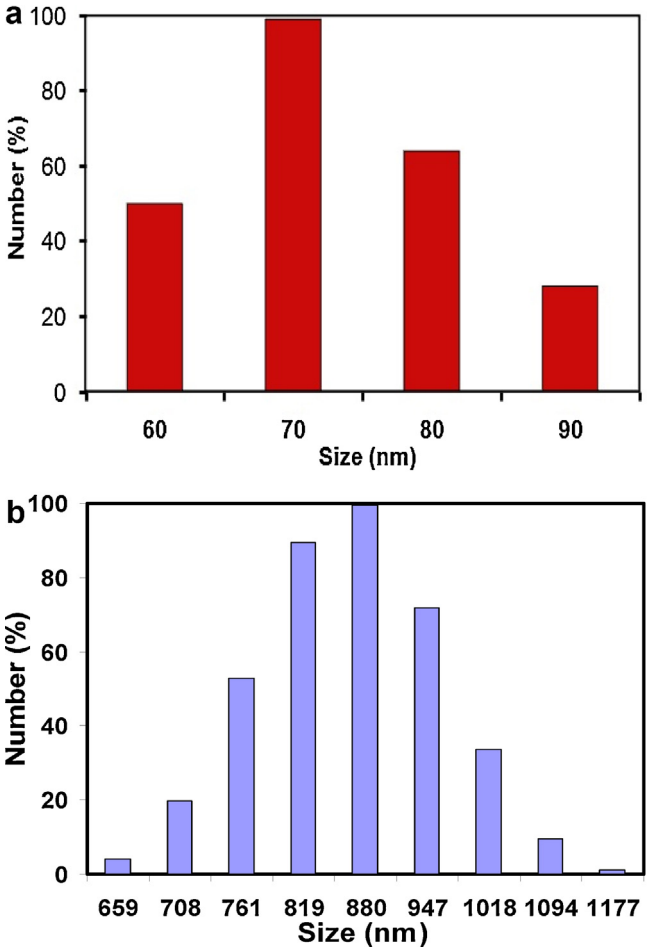

Fig. 6. (a) Particle size analysis of PTP/SnO_2 nano hybrid prepared by ultrasound assisted chemical oxidative polymerization. Particle size analysis of PTP/SnO_2 hybrid prepared via conventional chemical oxidative polymerization.

to be resolved by ultrasound as has been demonstrated for similar systems [46,47,24,48,49]. The formation of PTP encapsulated SnO_2 is due to the strong interaction between PTP and SnO_2. It is expected that due to ultrasound, uniform and homogeneous distribution of SnO_2 can be obtained and hence the ultrasonically synthesized hybrid composite is expected to give an excellent response [50,51].

The particle size distribution of PTP/SnO_2 hybrid prepared by ultrasound assisted and conventional chemical oxidative polymerization technique (in the absence of ultrasound) has been depicted in Fig. 6(a) and (b). The particle size of PTP/SnO_2 hybrid nanoparticles prepared using ultrasound assisted approach was found to be in the range 60–80 nm which is about 10 times lower as compared to that observed (over the range 659–1177 nm) in the case of conventional chemical oxidative polymerization method (without use of ultrasound). The average particle size of PTP/SnO_2 hybrid nanoparticles was 70 nm in the case of ultrasound assisted method whereas it was 834 nm for conventional chemical oxidative polymerization. The significant decrease in the particle size of PTP/SnO_2 hybrid nanoparticles is attributed to the enhanced micromixing, rapid nucleation, improved solute transfer rate and formation of large number of nuclei due to physical effects of the ultrasonic irradiation [12]. Due to the fast kinetics of ultrasound assisted

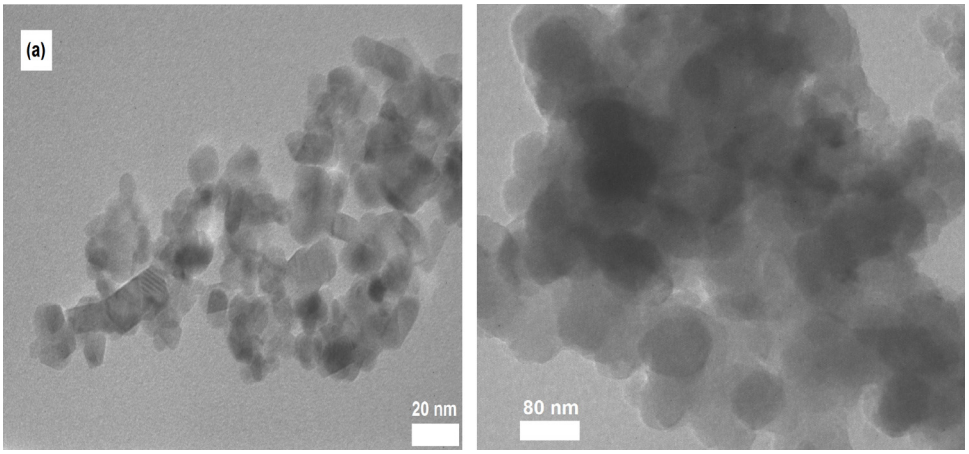

Fig. 5. (a) TEM image of SnO_2 prepared by ultrasound assisted. (b) TEM image of PPT/SnO_2 nano hybrid prepared by ultrasound assisted chemical oxidative polymerisation precipitation.

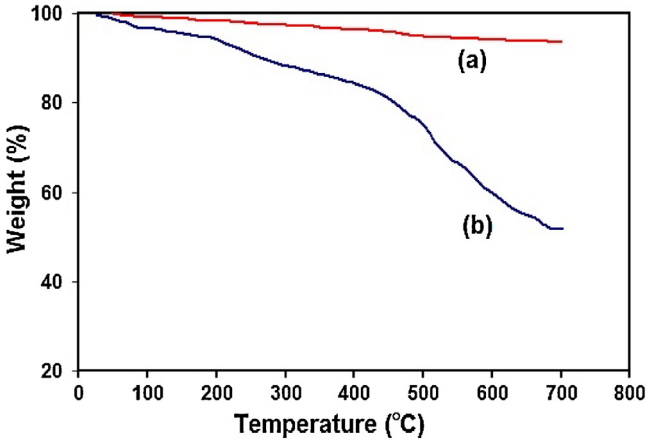

Fig. 7. Thermogravimetric analysis (TGA) of (a) SnO_2 and (b) PTP/SnO_2 nano hybrid.

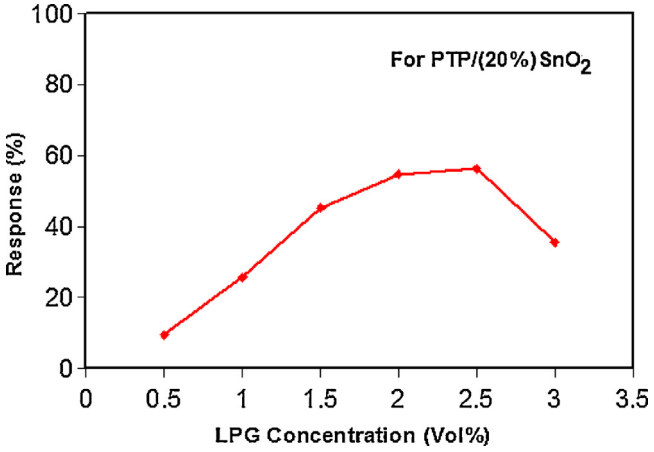

Fig. 8. Response of PTP/SnO_2 sensor as a function of the concentration of LPG gas (for PTP/(20%) SnO_2).

chemical oxidative polymerization, enough time is not provided for the growth of particle size which leads to reduction in particle size. The turbulence generated due to the ultrasound induced acoustic streaming [52,53] also helps in preventing the large growth of particles or induces breakage giving lower final size. Also delayed polymerization time in the case of conventional chemical oxidative polymerization (i.e. 100 min) is responsible for larger particle size of PTP/SnO_2 hybrid.

3.4. Thermal gravimetric analysis (TGA) of SnO_2 and PTP/SnO_2 hybrid nanocomposites

The results of thermogravimetric analysis (TGA) of nanosize SnO_2 and PTP/SnO_2 have been given in Fig. 7. It has been observed that the nanoparticles of SnO_2 (Fig. 7(a)) show the first step loss in weight at temperature less than or equal to 150 °C. It may be due to the removal of physically adsorbed water and volatile impurities present on SnO_2 nanoparticles. In the second step chemically adsorbed water is removed from the system at temperature greater than 150 °C and decomposition of NH_4^+ occurs at 390 °C. During this stage, the weight loss occurs gradually. In the case of PTP/SnO_2 hybrid (Fig. 7(b)) gentle decomposition with 3% weight loss at 100 °C and 43% weight loss at 700 °C has been observed. Also at 200 and 400 °C, a higher weight loss is attributed to the possible degradation of the polythiophene.

The SnO_2 particles were comparatively stable in the range of 0–700 °C. The cavitation micro jets facilitate the formation of crystalline SnO_2 particles during precipitation, which has been confirmed from the X-ray diffraction analysis. The major weight loss in TGA curve of hybrid composite was due to PTP degradation. The binding between the polymer and SnO_2 shows the strong chemical interaction as inferred from FTIR results [54,55].

3.5. Gas sensing study of polythiophene–SnO_2 hybrid nanocomposites

The room temperature gas response to various concentrations of LPG gas was measured by recording the resistance of the pellet in air and in the presence of test gas. The initial resistance of the PTP sensor was observed in the range of several kilo-ohms, while the PTP/SnO_2 sensor showed a lower resistance. Thus, the PTP/SnO_2 hybrid nanocomposite showed an increased conductivity compared to the pure PTP film, inferring that an increase in the conjugation length in PTP chains and the effective charge transfer between PTP and SnO_2 may result in an increase in the conductivity [54–57]. In addition, the improved contact between each grain via grain boundary may enhance the conductivity [58]. The LPG response of the PTP/SnO_2 hybrid at an applied potential of +2 V is depicted in Fig. 8. From this figure, it is concluded that the gas response is a function of LPG concentration. The gas response increased from 9.5% to 56.2% with an increase in concentration of LPG from 0.5 to 2.5 vol%. The relative response tends to increase initially with increasing concentrations possibly due to the availability of a large number of reactive species in the sensing layer. However, the slow increase in response at higher concentration may be due to limited availability of surface area with possible reaction sites on the surface of the film due to adsorption of the gas molecules [59]. The maximum gas response of 56.2% was observed at 2.5 vol%. The enhanced response of PTP/SnO_2 hybrid nanocomposite can be explained on the basis of the fact that p-type (polythiophene) and n-type SnO_2 may form a p–n junction. Also, the creation of positively charged depletion layer on the surface of n-type material (SnO_2) due to the inter particle electron migration from n-type (SnO_2) to p-type (PTP) at the heterojunction helps in yielding better response characteristics. The net result would be in terms of the reduction of the activation energy and enthalpy of physisorption for LPG [60–62]. At 3 vol% of LPG, the response decreased to 35.6%. This may be due to the formation of multilayer of LPG molecules on the interface of junction at the higher gas concentrations resulting in the saturation in gas response.

The response/recovery time is an important parameter used for characterizing a sensor. The response time is defined as the time taken by the sensor to attain 90% of the maximum increase in the resistance on exposure to the target gas. Similarly, the recovery time can be defined as the time to get back 90% of the maximum resistance when exposed to air. The variation of response and recovery times with different concentration of LPG at room temperature has been given in Fig. 9. It has been observed that the response time decreases from 196 to 94 s, while recovery time increases from 182 to 466 s with increasing LPG concentration from 0.5 to 2.5 vol%. The observed trends may be attributed to the presence of sufficient gas molecules at the pellet surface of nanocomposite for the reaction to occur. From the same graph, it is found that at higher concentrations of LPG, the recovery time was long. This may be due to the higher density of LPG and the fact that the reaction products do not leave the interface immediately after the reaction.

Fig. 10 indicates that the presence of SnO_2 nanoparticles significantly reduces the response time of PTP sensor for 2 to 2.5 vol% of LPG concentration. It can be seen that the response time is dependent on the SnO_2 concentration in the PTP/SnO_2 sensors. The response (at 2–2.5 vol% LPG) of the neat PTP sensor was recorded within 410–360 s, which is reduced to 340–310, 280–224, 156–110 and 124–94 for the PTP/SnO_2 sensor containing 5, 10, 15 and 20

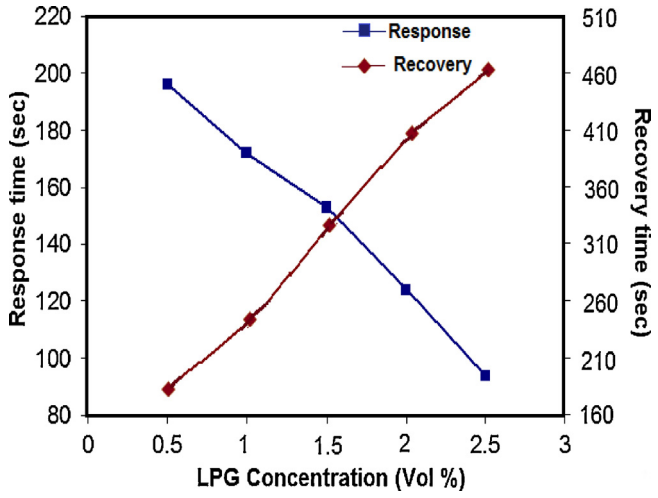

Fig. 9. Variation of response and recovery time of the PTP/SnO_2 hybrid sensor with LPG concentration (for PTP/(20%) SnO_2).

wt% of SnO_2, respectively. Thus, it can be established that the PTP/SnO_2 is more sensitive to LPG as compared to pure PTP. It indicates that different degree of interaction occurs between adsorbed LPG molecules and different sensors under the same experimental conditions. At higher concentrations of LPG, the diffusion rate is higher and sufficient quantities of gas molecules are available which reduces the response time.

3.5.1. LPG sensing mechanism of hybrid SnO_2/PTP

As already mentioned, pure PTP is a p-type semiconductor and the adsorption of LPG at PTP surface donates electrons and consequently its resistance increases. On the other hand, SnO_2 is an n-type semiconductor and its resistance decreases, when exposed to the reducing gas such as LPG. When hybrid PTP/SnO_2 nanocomposite is exposed to LPG, it exhibits the properties of p-type semiconductor, that is, its resistance increases on exposure to LPG. This observation suggests that the LPG sensing mechanism of the hybrid is governed by PTP, which is supported by TEM study. As revealed by TEM study, the SnO_2 nanoparticles are covered and interconnected with PTP in the nanocomposite and therefore, the active sites on the PTP backbone are largely accessible to LPG [62,63]. The response time of hybrid toward LPG is considerably lower than that of the pure PTP. The hybrid exhibits excellent LPG sensing characteristics than pure PTP, suggesting that the SnO_2 nanoparticles in the nanocomposite are also playing an active role in the sensing process.

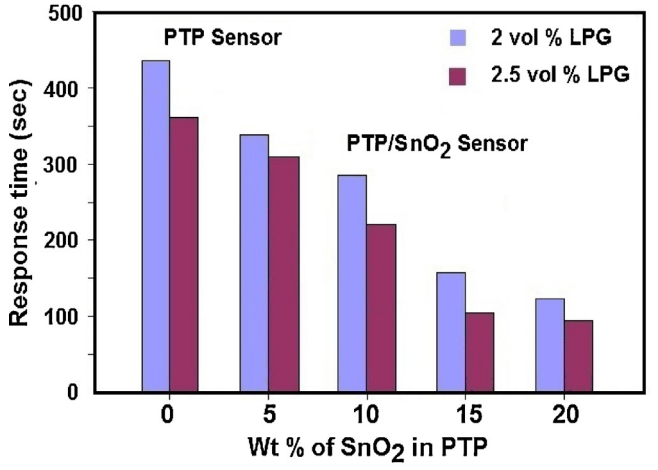

Fig. 10. Variation of response time as a function of different wt% of SnO_2 in the sensor at different LPG concentrations.

The schematic representation of the model based on the principle of formation of heterojunction barrier is depicted in Fig. 11 to explain the LPG sensing behavior of hybrid PTP/SnO_2 nanocomposite. When, the hybrid nanocomposite is exposed to the LPG, the LPG gas molecules are adsorbed preferentially on PTP and it leads to the interaction of LPG at the interface of p-PTP/n-SnO_2 heterojunction. The adsorption of LPG at PTP surface donates electrons and results in more negative acceptor ions on the p-side and hence there is a possibility of a wider space charge layer. As the surface of SnO_2 nanoparticles is generally covered with negatively charged adsorbed O-ions, an electron depletion layer is created on n-side of the junction. As a result, the carrier concentration of the heterojunction decreases and consequently, the potential barrier height of the heterojunction increases giving an increase in the resistance of the hybrid. Therefore, PTP identify LPG (receptor function) and both PTP and SnO_2 nanoparticles provide conducting path (transducer function) and hence the nanocomposite permits selective detection of LPG at room temperature.

3.5.2. Comparison of hybrid with other sensors

The combination of these two materials (conducting polymer and SnO_2) to give a hybrid nanocomposite can lead to a synergistic effect, which are helpful for improving the sensor properties such as thermal stability, lower operating temperature, and fast response and recovery. To establish the utility of hybrid sensors, it is essential to compare the response characteristics of the hybrid sensor with some of the reported literature illustrations.

Song et al. [62] synthesized polypyrrole/$ZnSnO_3$ nanocomposite which were prepared by a simple in situ chemical polymerization method. It has been reported that these nanocomposites exhibited a higher response upto 90% for 1000 ppm NH_3 gas. Xu et al. [49] reported that the NO_2 sensor based on PTP-coated SnO_2 hollow spheres exhibited higher gas response and shorter recovery time for detecting NO_2 at ppm levels at 90 °C in comparison with the sensor based on pure PTP. Dhawale et al. [63] fabricated p-polyaniline/n-ZnO thin film heterojunction sensor for room temperature LPG detection via electrodepositing polyaniline on chemical bath deposited ZnO film. The heterojunction sensor has quick and high response toward LPG as compared to N_2 and CO_2 and exhibited maximum response of 81% upon exposure to 1040 ppm of LPG. Deshpande et al. [64] synthesized the SnO_2-intercalated PANI nanocomposite, which showed better sensitivity to ammonia gas at room temperature than SnO_2 with the response and recovery times of 12–15 s and 80 s for 300 ppm ammonia gas, respectively. However, pure PANI exhibited better sensitivity to ammonia than SnO_2-intercalated PANI nanocomposite with relatively fast response (8–10 s) and slow recovery (160 s). Kong et al. [65] recently reported the synthesis of SnO_2–PTP composites and studied their NO_2 sensing properties at low operating temperatures, which were reported to be better than SnO_2. Patil et al. [66] investigated Poly(*o*-anisidine)-tin oxide (POA–SnO_2) nanocomposites via in situ chemical polymerization of *o*-anisidine in presence of SnO_2 nanoparticles. The POA–SnO_2 nanocomposite shows better LPG sensing properties than that observed for the pure POA. The nanocomposite with 50 wt% SnO_2 exhibit excellent LPG sensing characteristics at the operating temperature of 100 °C such as higher relative gas response (~23.47% to 3.4% of LPG), extremely rapid response (~6 s), fast recovery (~33 s), good reproducibility, and remarkable selectivity. In contrast, the present LPG sensor based on PTP/SnO_2 hybrid has a relative LPG response of 56.2% for 2.5 vol% LPG at room temperature as shown in Fig. 8. Also it has a response time of 94 s and recovery time of 466 s for 2.5 vol% at PTP/(20%) SnO_2, respectively. Also PTP/SnO_2 hybrid nanocomposites have better LPG sensing characteristics than the

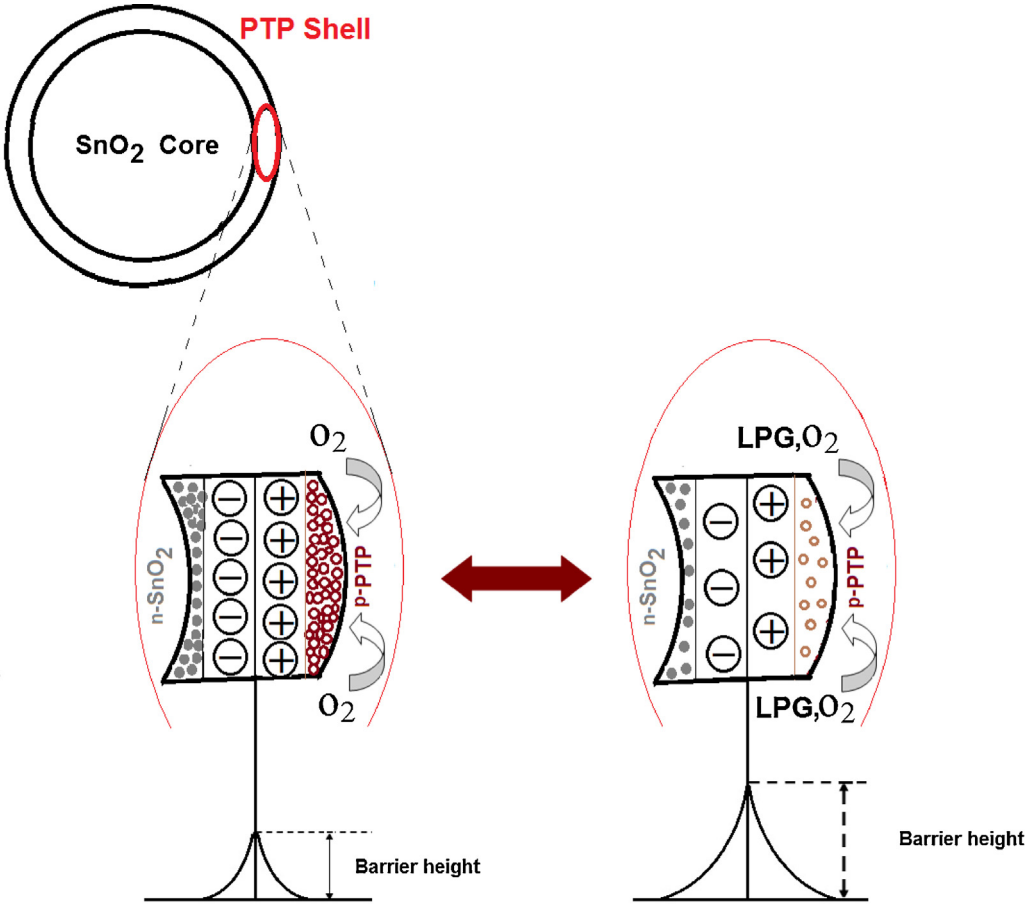

Fig. 11. Schematic representation of LPG sensing model for PTP/SnO_2 nano hybrid.

semiconducting metal oxide based LPG sensors reported in the literature [66–70] and can overcome the shortcomings of longer response time, slow recovery and lack of selectivity of PTP and requirement of higher operating temperature of SnO_2, thus presenting very promising sensing material for the fabrication of LPG sensors operating at low temperatures.

4. Conclusions

Inorganic-organic hybrid materials of SnO_2 nanoparticles coated by PTP have been successfully prepared through an ultrasound assisted in situ chemical oxidative polymerization of thiophene in the presence of SnO_2 nanoparticles. The presence of ultrasonic irradiation creates conditions suitable for intense micromixing resulting into lower sizes of the final composite as established using comparisons with experiments based on the conventional approach in the absence of ultrasound. XRD, FTIR and TEM results showed that there is a certain synergetic interaction between the SnO_2 nanoparticles and polythiophene. Uniform encapsulation of SnO_2 particles into the PTP improves the LPG sensing performance, implying the potential sensor applications of the hybrids. The maximum sensing capability along with better long term stability was observed for the sensor containing 20 wt% SnO_2.

Acknowledgment

Mr Shrikant S. Barkade acknowledges Chemical Engineering Department of Institute of Chemical Technology Mumbai for summer research Training in 2011 and Chemical Engineering Department, Sinhgad College of Engineering Pune and Department of Chemical Technology North Maharashtra University Jalgaon.

References

[1] Y. Bai, N.L. Abbott, Recent advances in colloidal and interfacial phenomena involving liquid crystals, Langmuir 27 (2011) 5719–5738.
[2] G. Kickelbick, D. Holzinger, C. Brick, G. Trimmel, E. Moons, Hybrid inorganic–organic core–shell nanoparticles from surface-functionalized titanium, zirconium, and vanadium oxo clusters, Chemistry of Materials 14 (2002) 4382–4389.
[3] V. Mittal, Sedimentation analysis of organic–inorganic hybrid colloids, Colloid and Polymer 288 (2010) 621–630.
[4] F. Caruso, R.A. Caruso, H. Mohwald, Nanoengineering of inorganic and hybrid hollow spheres by colloidal templating, Science 282 (1998) 1111–1114.
[5] K.S. Suslick, G.J. Price, Applications of ultrasound to materials chemistry, Annual Review of Materials Research 29 (1999) 295–326.
[6] G.J. Price, Recent developments in sonochemical polymerisation, Ultrasonics Sonochemistry 10 (2003) 277–283.
[7] B.M. Teo, S.W. Prescott, M. Ashokkumar, F. Grieser, Ultrasound initiated miniemulsion polymerization of methacrylate monomers, Ultrasonics Sonochemistry 15 (2008) 89–94.
[8] B.A. Bhanvase, D.V. Pinjari, P.R. Gogate, S.H. Sonawane, A.B. Pandit, Process intensification of encapsulation of functionalized $CaCO_3$ nanoparticles using ultrasound assisted emulsion polymerization, Chemical Engineering and Processing 50 (2011) 1160–1168.
[9] K. Zhang, B. Park, F. Fang, H. Choi, Sonochemical preparation of polymer nanocomposites, Molecules 14 (2009) 2095–2110.
[10] L.H. Thompson, L.K. Doraiswamy, Sonochemistry: science and engineering, Industrial & Engineering Chemistry Research 38 (1999) 1215–1249.
[11] F. Contamine, F. Faid, A.M. Wilhelm, J. Berlan, H. Delmas, Chemical reactions under ultrasound: discrimination of chemical and physical effects, Chemical Engineering Science 49 (1994) 5865–5873.
[12] P.R. Gogate, V.S. Sutkar, A.B. Pandit, Sonochemical reactors: important design and scale up considerations with a special emphasis on heterogeneous systems, Chemical Engineering Journal 166 (2011) 1066–1082.
[13] C. Gong, D.P. Hart, Ultrasound induced cavitation and sonochemical yields, Journal of the Acoustical Society of America 104 (1998) 1–16.

[14] P.R. Gogate, R.K. Tayal, A.B. Pandit, Cavitation: a technology on the horizon, Current Science 91 (1) (2006) 35–46.
[15] M.K. Ram, O. Yavuz, M. Aldissi, NO_2 gas sensing based on ordered ultrathin films of conducting polymer and its nanocomposite, Synthetic Metals 151 (2005) 77–84.
[16] D.S. Dhawale, R.R. Salunkhe, U.M. Patil, K.V. Gurav, A.M. More, C.D. Lokhande, Room temperature liquefied petroleum gas (LPG) sensor based on *p*-polyaniline/*n*-TiO_2 heterojunction, Sensors and Actuators B: Chemical 134 (2008) 988–992.
[17] M.E. Nicho, M. Trejo, A.G. Valenzaela, J.M. Saniger, J. Palacios, H. Hu, Polyaniline composite coatings interrogated by a nulling optical bridge for sensing low concentration of ammonia gas, Sensors and Actuators B: Chemical 76 (2001) 18–24.
[18] K. Hosono, I. Matsubara, N. Murayama, S. Woosuck, N. Izu, Synthesis of polypyrrole/MoO_3 hybrid thin film and their volatile organic compound gas-sensing properties, Chemistry of Materials 17 (2005) 349–354.
[19] D.V. Pinjari, A.B. Pandit, Room temperature synthesis of crystalline CeO_2 nanopowder: advantage of sonochemical method over conventional method, Ultrasonics Sonochemistry 18 (2011) 1118–1123.
[20] A. Hassanjani-Roshana, M.R. Vaezi, A. Shokuhfar, Z. Rajabali, Synthesis of iron oxide nanoparticles via sonochemical method and their characterization, Particuology 9 (2011) 95–99.
[21] M.S.Y. Parast, A. Morsali, Sonochemical-assisted synthesis of nano-structured indium(III) hydroxide and oxide, Ultrasonics Sonochemistry 18 (2011) 375–381.
[22] S.R. Shirsath, D.V. Pinjari, P.R. Gogate, S.H. Sonawane, A.B. Pandit, Ultrasound assisted synthesis of doped TiO_2 nano-particles: characterization and comparison of effectiveness for photocatalytic oxidation of dyestuff effluent, Ultrasonics Sonochemistry 20 (2013) 277–286.
[23] M. Sivakumar, A. Gedanken, A sonochemical method for the synthesis of polyaniline and Au–polyaniline composites using H_2O_2 for enhancing rate and yield, Synthetic Metals 148 (2005) 301–306.
[24] J. Park, M. Atobe, T. Fuchigami, Sonochemical synthesis of conducting polymer–metal nanoparticles nanocomposite, Electrochimica Acta 51 (2005) 849–854.
[25] E. Kowsari, G. Faragh, Ultrasound and ionic-liquid-assisted synthesis and characterization of polyaniline/Y_2O_3 nanocomposite with controlled conductivity, Ultrasonics Sonochemistry 17 (2010) 718–725.
[26] Y. Azizian-Kalandaragh, A. Khodayari, M. Behboudnia, Ultrasound-assisted synthesis of ZnO semiconductor nanostructures, Materials Science in Semiconductor Processing 12 (2009) 142–145.
[27] B.A. Bhanvase, D.V. Pinjari, P.R. Gogate, S.H. Sonawane, A.B. Pandit, Synthesis of exfoliated poly(styrene-*co*-methyl methacrylate)/montmorillonite nanocomposite using ultrasound assisted in situ emulsion copolymerization, Chemical Engineering Journal 181 (2012) 770–778.
[28] K.F. O'Driscoll, A.U. Sridharan, Effect of ultrasound on free-radical polymerization in a continuous stirred tank reactor, Journal of Polymer Science Part A: Polymer Chemistry 11 (2003) 1111–1117.
[29] X. Ai, N. Anderson, J. Guo, J. Kowalik, L.M. Tolbert, T. Lian, Ultrafast photoinduced charge separation dynamics in polythiophene/SnO_2 nanocomposites, The Journal of Physical Chemistry B 110 (2006) 25496–25503.
[30] S.B. Patil, A.K. Singh, Solution growth nanocrystalline ZnO thin films for UV emission and LPG sensing, Journal of Materials Science 45 (2010) 5204–5210.
[31] B. Bittmann, F. Haupert, A.K. Schlarb, Preparation of TiO_2/epoxy nanocomposites by ultrasonic dispersion and their structure property relationship, Ultrasonics Sonochemistry 18 (2011) 120–126.
[32] H. Xia, Qi Wang, Ultrasonic irradiation: a novel approach to prepare conductive polyaniline/nanocrystalline titanium oxide composites, Chemistry of Materials 14 (2002) 2158–2165.
[33] B.M. Teo, F. Chen, T.A. Hatton, F. Grieser, M. Ashokkumar, Novel one-pot synthesis of magnetite latex nanoparticles by ultrasound irradiation, Langmuir 25 (2009) 2593–2595.
[34] J. Zhang, S. Wang, M. Xu, Y. Wang, H. Xia, S. Zhang, X. Guo, S. Wu, Polypyrrole-coated SnO_2hollow spheres and their application for ammonia sensor, The Journal of Physical Chemistry C 113 (2009) 1662–1665.
[35] M.G. Han, S.H. Foulger, Crystalline colloidal arrays composed of poly-(3,4-ethylenedioxythiophene)-coated polystyrene particles with a stop band in the visible regime, Advanced Materials 16 (2004) 231–234.
[36] F. Zhu, S.B. Xu, L. Jiang, K.L. Pan, Y. Dan, Synthesis and characterization of polythiophene/titanium dioxide composites, Reactive and Functional Polymers 68 (2008) 1492–1498.
[37] D.N. Srivastava, S. Chappel, O. Palchik, A. Zaban, A. Gedanken, Sonochemical synthesis of mesoporous tin oxide, Langmuir 18 (2002) 4160–4164.
[38] K.R. Reddy, W. Park, B.C. Sin, J. Noh, Y. Lee, Synthesis of electrically conductive and superparamagnetic monodispersed iron oxide-conjugated polymer composite nanoparticles by in-situ chemical oxidative polymerization, Journal of Colloid and Interface Science 335 (2009) 34–39.
[39] X. Ai, N. Anderson, J.C. Guo, J. Kowalik, L.M. Tolbert, T.Q. Lian, Ultrafast photoinduced charge separation dynamics in polythiophene/SnO_2 nanocomposites, The Journal of Physical Chemistry B 110 (2006) 25496–25503.
[40] J. Wang, Y. Hu, B. Li, Z. Gui, Z. Chen, Preparation of polyacrylamide and gamma-zirconium phosphate nanocomposites by intercalative polymerization, Ultrasonics Sonochemistry 11 (2004) 301–306.
[41] Z. Guo, T. Pereira, O. Choi, Y. Wang, H.T. Hahn, Surface functionalized alumina nanoparticle filled polymeric nanocomposites with enhanced mechanical properties, Journal of Materials Chemistry 16 (2006) 2800–2808.
[42] X.Y. Yuan, L.L. Zou, C.C. Liao, J.W. Dai, Improved properties of chemically modified graphene/poly(methyl methacrylate) nanocomposites via a facile in-situ bulk polymerization, Express Polymer Letters 6 (2012) 847–858.
[43] M.R. Karim, C.J. Lee, M.S. Lee, Synthesis and characterization of conducting polythiophene/carbon nanotubes composites, Journal of Polymer Science Part A: Polymer Chemistry 44 (2006) 5283–5290.
[44] Y.N. Li, G. Vamvounis, S. Holdcroft, Tuning optical properties and enhancing solid-state emission of poly(thiophene)s by molecular control: a post functionalization approach, Macromolecules 35 (2002) 6900–6906.
[45] M. Xu, J. Zhang, S. Wang, X. Guo, H. Xia, Y. Wang, S. Zhang, W. Huang, S. Wu, Gas sensing properties of SnO_2 hollow spheres/polythiophene inorganic–organic hybrids, Sensors and Actuators B: Chemical 146 (2010) 8–13.
[46] B. Bittmann, F. Haupert, A.K. Schlarb, Preparation of TiO_2/epoxy nanocomposites by ultrasonic dispersion and their structure property relationship, Ultrasonic Sonochemistry 18 (2011) 120–126.
[47] H. Xia, Qi Wang, Ultrasonic irradiation: a novel approach to prepare conductive polyaniline/nanocrystalline titanium oxide composites, Chemistry of Materials 14 (2002) 2158–2165.
[48] B.A. Rozenberga, R. Tenne, Polymer-assisted fabrication of nanoparticles and nanocomposites, Progress in Polymer Science 33 (2008) 40–112.
[49] Z. Kai, F. Qiang, H. Yuhong, Z. Dehui, Encapsulation of inorganic particles by dispersion polymerization through ultrasonic irradiation, Science in China Series B: Chemistry 48 (2005) 545–552.
[50] S. Zhu, J. Guo, J. Dong, Z. Cui, T. Lu, C. Zhu, D. Zhang, J. Ma, Sonochemical fabrication of Fe_3O_4 nanoparticles on reduced graphene oxide for biosensors, Ultrasonic Sonochemistry 20 (2013) 872–880.
[51] Q. Wang, X. Cui, J. Chen, X. Zheng, C. Liu, T. Xue, H. Wang, Z. Jin, L. Qiao, W. Zheng, Well-dispersed palladium nanoparticles on graphene oxide as a non-enzymatic glucose sensor, RSC Advances 2 (2012) 6245–6249.
[52] A. Kumar, P.R. Gogate, A.B. Pandit, Mapping of acoustic streaming in sonochemical reactors, Industrial Engineering Chemistry Research 46 (2007) 4368–4373.
[53] N.P. Vichare, V.Y. Dindore, P.R. Gogate, A.B. Pandit, Mixing time analysis of a sonochemical reactor, Ultrasonics Sonochemistry 8 (2001) 23–33.
[54] N. Ballav, M. Biswas, Conducting composites of polythiophene and polyfuran with acetylene black, Polymer International 54 (2005) 725–729.
[55] L. Yuan, J. Wang, S.Y. Chew, J. Chen, Z.P. Guo, L. Zhao, K. Konstantinov, H.K. Liu, Synthesis and characterization of SnO_2–polypyrrole composite for lithium ion battery, Journal of Power Sources 174 (2007) 1183–1187.
[56] S.J. Su, N. Kuramoto, Processable polyaniline–titanium dioxide nanocomposite: effect of titanium dioxide on the conductivity, Synthetic Metals 114 (2000) 147–153.
[57] W. Feng, X.D. Bai, Y.Q. Lian, J. Liang, X.G. Wang, K. Yoshino, Well aligned polyaniline/carbon-nanotube composite films grown by in-situ aniline polymerization, Carbon 41 (2003) 1551–1557.
[58] R.P. Tandon, M.R. Tripathy, A.K. Arora, S. Hotchandani, Gas and humidity response of iron oxide–polypyrrole nanocomposites, Sensors and Actuators B: Chemical 114 (2006) 768–773.
[59] D.S. Sutar, N. Padma, D.K. Aswal, S.K. Deshpande, S.K. Gupta, J.V. Yakhmi, Preparation of nanofibrous polyaniline films and their application as ammonia gas sensor, Sensors and Actuators B: Chemical 128 (2007) 286–292.
[60] H. Tai, Y. Juang, G. Xie, J. Yu, X. Chen, Fabrication and gas sensitivity of polyaniline–titanium dioxide nanocomposite thin film, Sensors and Actuators B: Chemical 125 (2007) 644–650.
[61] Q. Tang, L. Lin, X. Zhao, K. Huang, J. Wu, p–n Heterojunction on ordered ZnO nanowires/polyaniline microrods double array, Langmuir 28 (2012) 3972–3978.
[62] P. Song, Q. Wang, Z. Yang, Ammonia gas sensor based on PPy/$ZnSnO_3$ nanocomposites, Materials Letters 65 (2011) 430–432.
[63] D.S. Dhawale, D.P. Dubal, A.M. More, T.P. Gujar, C.D. Lokhande, Room temperature liquefied petroleum gas (LPG) sensor, Sensors and Actuators B: Chemical 147 (2010) 488–494.
[64] N. Deshpande, Y. Gudage, R. Sharma, J. Vyas, J. Kim, Y. Lee, Studies on tin oxide-intercalated polyaniline nanocomposite for ammonia gas sensing applications, Sensors and Actuators B: Chemical 138 (2009) 76–84.
[65] F. Kong, Y. Wang, J. Zhang, H. Xia, B. Zhu, Y. Wang, S. Wang, S. Wu, The preparation and gas sensitivity study of polythiophene/SnO_2 composites, Material Science and Engineering: B 150 (2008) 6–11.
[66] D. Patil, K. Kolhe, H.S. Potdar, P. Patil, Investigation of poly(*o*-anisidine)–SnO_2 nanocomposites for fabrication of low temperature operative liquefied petroleum gas sensor, Journal of Applied Physics 110 (2011) 124501–124508.
[67] G.N. Chaudhari, D.R. Bambole, A.B. Bodade, Structural and gas sensing behavior of nanocrystalline $BaTiO_3$ based liquid petroleum gas sensors, Vacuum 81 (2006) 251–256.
[68] Z. Jiao, G.G. Ye, F. Chen, M. Li, J. Liu, Preparation of ZnGa2O4 nano crystals by spray coprecipitation and its gas sensitive characteristics, Sensors (2002) 71–78.
[69] P.P. Sahay, R.K. Nath, Al-doped zinc oxide thin films for liquid petroleum gas (LPG) sensors, Sensors and Actuators B: Chemical 133 (2008) 222–227.
[70] R.R. Salunkhe, D.S. Dhawale, U.M. Patil, C.D. Lokhande, Improved response of CdO nanorods towards liquefied petroleum gas (LPG): effect of Pd sensitization, Sensors and Actuators B: Chemical 136 (2009) 39–44.